Biochemical Pharmacology 83 (2012) 355–367

Contents lists available at SciVerse ScienceDirect

Biochemical Pharmacology

journal homepage: www.elsevier.com/locate/biochempharm

Hsp90 inhibitors sensitise human colon cancer cells to topoisomerase I poisons by depletion of key anti-apoptotic and cell cycle checkpoint proteins

Anne V. McNamara [1], Monica Barclay [2], Alastair J.M. Watson [3], John R. Jenkins *

The University of Liverpool, Institute of Translational Medicine, Department of Gastroenterology, The Henry Wellcome Laboratory, Crown Street, Liverpool, L69 3GE, UK

ARTICLE INFO

Article history:
Received 3 October 2011
Accepted 18 November 2011
Available online 28 November 2011

Keywords:
Topoisomerase I
Hsp90
P53
Irinotecan
Topotecan
17AAG

ABSTRACT

Hsp90 and topoisomerase I are both targets for chemotherapeutic agents. Topoisomerase I poisons are standard clinical treatments, whilst Hsp90 inhibitors are progressing through clinical trials. We have demonstrated that when an Hsp90 inhibitor and topoisomerase I poison are combined they produce a synergistic increase in apoptosis in both $p53^{+/+}$ and $p53^{-/-}$ HCT116 human colon cancer cells. Lack of p53 is associated with an increase in sensitivity to the combination treatment; $p53^{+/+}$ cells treated with the topoisomerase I poison topotecan (TPT) arrest at G2, whereas in $p53^{-/-}$ cells the additional presence of the Hsp90 inhibitor geldanamycin (GA) selectively abrogates the G2M checkpoint. More importantly we report that there is a common underlying p53-independent mechanism behind the observed synergistic combined drug effect. We show that concurrent treatment with GA and TPT is able to reverse TPT induced up-regulation of the anti-apoptotic protein Bcl2 in both $p53^{+/+}$ and $p53^{-/-}$ HCT116 cells. The data suggests that inhibition of Hsp90 mediates down-regulation of Bcl2 following the combination treatment and cause a synergistic increase in apoptosis in both $p53^{+/+}$ and $p53^{-/-}$ HCT116 cells; $p53^{-/-}$ HCT116 cells are more sensitive to the treatment because they also fail to arrest at G2 in the cell cycle.

1. Introduction

DNA topoisomerases are essential enzymes, allowing DNA strands or double helices to pass through one another resolving the topological problems of DNA in replication, transcription and other cellular transactions [1]. Topoisomerases are classified on the basis of the number of DNA strands they cleave, the intermediate phosphodiester generated and/or their structures. Due to their vital role, they are the targets of a number of chemotherapeutic agents, specifically topoisomerase cytotoxins. The main mechanism by which these poisons induce cell cycle S-phase specific death is thought to be by the formation of cleavable complexes, which are converted to double stranded (ds) DNA breaks upon collision with a replication fork (topoisomerase I, [2,3]) (topoisomerase II, [4]). Previous work from our laboratory, in colorectal cancer models, demonstrated that cell lines both $p53^{+/+}$ and $p53^{-/-}$ and xenografts are sensitised to topoisomerase II poisons, such as etoposide, if an Hsp90 inhibitor is used as part of a combination treatment [5]. We have also presented data supporting our proposed mechanism, demonstrating that there is an increase in topoisomerase II mediated DNA damage with these combination treatments [6].

Heat shock protein 90 (Hsp90) is highly conserved from yeast to mammalian cells and is an essential molecular chaperone accounting for between 1 and 2% of total cellular protein. It plays a key role in the folding, activation and assembly of a range of proteins including many involved in signal transduction and cell cycle control (reviewed in [7]. Hsp90 is abundant in healthy tissues so initially it was unclear why Hsp90 inhibitors were able to selectively kill tumour cells; in normal cells latent Hsp90 is present in its uncomplexed state whereas in tumour cells Hsp90 is present almost entirely in its multi-chaperone state. It has been proposed that during malignant progression Hsp90 becomes completely utilised in its high affinity complex aided by the binding of co-chaperones. It also participates in the activation and stabilisation of oncoproteins [8]. This conformational shift appears to partly explain the 100-fold increase in Hsp90 binding affinity for the Hsp90 inhibitor, 17-allylalamino-17demethoxy-geldanamycin (17-AAG) in tumour cells compared to Hsp90 in normal cells [8]. Hsp90 client proteins include many oncogenic signalling proteins, such as mutant p53 and AKT; and clients have been described as contributing to all ten hallmarks of cancer [9].

* Corresponding author. Tel.: +44 151 794 6828; fax: +44 151 794 6825.
E-mail address: john.jenkins@liverpool.ac.uk (J.R. Jenkins).
[1] Present address: Faculty of Life Sciences, Michael Smith Building, The University of Manchester, Oxford Road, Manchester, M13 9PT, UK.
[2] Present address: Faculty of Science, School of Sport and Exercise Sciences, Liverpool JMU. Henry Cotton Campus, Room 1.12a, 15-21 Webster Street, Liverpool, Merseyside, L3 2ET, UK.
[3] Present address: Norwich Medical School, University of East Anglia, Norwich Research Park, NR4 7TJ, UK.

0006-2952/$ – see front matter © 2011 Elsevier Inc. All rights reserved.
doi:10.1016/j.bcp.2011.11.017

Inhibition of Hsp90 causes degradation, activation or maintenance in an inactive form of its client proteins and may therefore affect numerous signalling pathways, thus it is not surprising that Hsp90 is seen as a promising target for anti cancer treatments [10].

The topoisomerase I poisons, routinely used clinically are derivatives of camptothecin (CPT), irinotecan (IRT) and topotecan (TPT), for the treatment of metastatic colorectal cancer and ovarian cancers respectively [11]. However there are several limitations affecting their use. Side effects such as leucopaenia and severe diarrhoea can limit the dose that can be safely administered to patients [12] and in addition, tumours can develop resistance to drugs.

Topoisomerase I mediated DNA damage leads to activation of the S and G2 cell cycle checkpoints as well as the p53 pathways [13,14], reviewed in [15]. However, interpretation of these pathways is complicated due to the different mechanisms involved in cell cycle inhibition; these in turn vary according to concentrations of topoisomerase I poisons. Depending on the dose of topoisomerase I poison and the cell type, different checkpoints have been found to be activated [16]. Treatment with low dose concentrations of topoisomerase I poisons, which are therapeutically achievable, results in S phase arrest followed by a reversible G2 arrest; whereas higher doses lead to an increased S phase arrest followed by arrest at G2 [17–19]. These dose-dependent effects of topoisomerase I poisons have been suggested to be a consequence of changes in gene expression patterns and cell cycle response [19,20].

Inhibitors targeting both topoisomerase I and Hsp90 (or the Hsp90 client protein, Chk1) have been assayed by a number of groups. However. However the results have been contradictory. Treatment combining gemcitabine (arguably a topoisomerase I poison [21]) and the Chk1 inhibitor UCN-01 in HeLa, OVCAR3 and ML-1 cells (human cervical, myeloblastic leukaemia and ovarian carcinoma cells respectively) was found to be additive [22]; combining TPT and UCN-01 also had an additive effect on breast cancer derived cells with mutant or inactive p53 [23]; combined CPT and UCN-01 treatment was found to cause an increase in DNA damage in $p53^{-/-}$ HCT116 cells compared to their wild type counterparts [2]. In addition, synergy following dual Hsp90 and topoisomerase I inhibition with 17AAG and the active metabolite of IRT, SN-38, was demonstrated in $p53^{-/-}$ HCT116 (human colon adenocarcinoma) cells, whilst in $p53^{+/+}$ HCT116 cells the combination was found to be antagonistic. In contrast, synergy was observed in $p53^{+/+}$ HCT116 cells in addition to HeLa and T98G (human glioblastoma cells) when combining 17AAG with SN-38, and broadened the potential mechanism to more than simply removal of Chk1 [25]. This highlights the very important point that Hsp90 inhibition results in the simultaneous degradation of numerous proteins.

Many of these studies used the widely established pair of isogenic cell lines HCT116 wild type ($^{+/+}$) and knock out ($^{-/-}$) for p53. We therefore used these cells as our model cell line, with the aim of dissecting the mechanism underlying combinations of clinically effective topoisomerase I poisons with Hsp90 inhibitors. We describe a common underlying p53 independent mechanism behind the observed combination synergistic drug effect. We show that concurrent treatment with a Hsp90 inhibitor (GA) and topoisomerase I poison TPT is able to reverse TPT induced up-regulation of the anti-apoptotic protein Bcl2.

2. Materials and methods

2.1. Cell lines

The isogenic human colon cancer cell lines, HCT116 p53 wild type ($^{+/+}$) and p53 knock out ($^{-/-}$) were a kind gift from Prof. B. Vogelstein (The John Hopkins Medical Institutions, Baltimore, MD, USA). Cells were maintained in McCoys 5A medium (Sigma, UK) supplemented with 10% foetal calf serum (Life Technologies, UK) at 37 °C in a 5% CO_2 enriched humidified environment.

2.2. Drugs

Hycamptin® (topotecan) and Camptosar® (irinotecan) were kind gifts from the Oncology Unit, Clatterbridge hospital, Wirral Trust Hospitals, UK. 17-AAG and geldanamycin were kind gifts from Dr. R.J. Schultz, Drug Synthesis and Chemistry Branch, Developmental Therapeutics Program, National Cancer Institute (Rockville, MD, USA). Geldanamycin was also obtained from Tocris Cookson Ltd. (Avonmouth, UK) and radicicol was obtained from Sigma–Aldrich Company Ltd. (St. Louis, USA).

2.3. Immunoblotting

HCT116 whole cell extracts were prepared by lysing cells in RIPA buffer (425 mM NaCl (Sigma, UK), 1% (v/v) IGEPAL CA-630 (Sigma, UK), 1 mM EDTA (Sigma, UK), 5% (w/v) deoxycholate (Sigma, UK), 50 mM Tris (Sigma, UK) pH 8.0, 0.1% (w/v) SDS (Sigma, UK), 10 mM sodium fluoride (Sigma, UK), 0.5 mM sodium orthovanadate (Sigma, UK)) containing the protease inhibitor cocktail III (Calbiochem, UK). Cells were incubated on ice for 30 min and cleared by sonication and centrifugation at 14,000 × *g* for 30 min at 4 °C. Whole cell extracts were separated by 10% SDS–PAGE under reducing conditions and blotted onto Protran® nitrocellulose membrane (Schleicher and Schuell UK Ltd., London, UK). Blots were probed with appropriate primary antibodies and the secondary antibodies conjugated with horse radish peroxidase (DAKOCytomation Ltd. Ely, UK) detection was by Supersignal® West Dura Extended Substrate (Perbio Science UK Ltd., Tattenhall, UK) and imaged using a Fluor-STM bioimager (Bio-Rad Laboratories Ltd., Hemel Hempstead, UK).

2.4. Antibodies

Mouse anti-human Pan actin, (LabVision Runcorn, UK), Mouse anti-human Bcl2 oncoprotein Clone 124, (Sigma, UK); Rat anti-human Apaf1 (Upstate, UK).

2.5. Growth inhibition assay

For growth inhibition studies the sulforhodamine B (Sigma, UK) assay was performed as described previously [5]. In brief, 3×10^3 cells per well were seeded into 96-well microtitre plates allowed to adhere overnight and then drugs were added in 6 replicate wells for a period of up to 7 days. At fixed daily time points cells were fixed with 3:1 methanol (Sigma, UK):acetic acid (Sigma, UK), stained with 0.4% (w/v) sulforhodamine B (SRB) and absorbance measured at 570 nm. The mean OD of treated cells was plotted against time (days).

2.6. Clonogenic assay

Cells were seeded at 1×10^3 cells per well in 6 well plates and allowed to adhere overnight. The cells were then exposed to the drugs for 1 h and reincubated in fresh media for 10 days to allow colony formation. Colonies were fixed in 70% methanol and stained with 0.2% (w/v) crystal violet/70% ethanol. The numbers of colonies formed of >50 cells each were counted. Experiments were performed independently three times with each concentration having six replicates.

2.7. Bi-parameter flow cytometry

Cells were seeded at 3×10^6 cells per 10 cm culture dish and allowed to adhere overnight. The cells were then treated with TPT

(213 nM) and GA (1.3 μM) either concurrently or as single agents over a 24 h period. Adherent cells were harvested at specific time points by trypsinisation and combined with floating cells. Cells were then fixed and antibody stained as described below.

2.8. Histone H3 (ser^{10})/PI and Bcl2/PI

Cells were fixed with chilled 70% ethanol. 1.5×10^6 fixed cells were resuspended in 0.25% Triton X-100 in PBS and incubated on ice for 15 min. Cells were then resuspended in 100 μl of PBS containing 1% BSA and 0.75 μl of anti phosphorylated histone H3 (Upstate Biotechnology) or 5 μl of anti-human Bcl2 antibody and incubated at room temperature for 3 h using a rotary mixer. Cells were then washed with 1% BSA in PBS and resuspended in 200 μl of 1% BSA in PBS containing 1 μl FITC conjugated goat anti-rabbit IgG antibody (Jackson Immunolabs) and incubated at room temperature for 30 min using a rotary mixer, protected from light. After washing with 1% BSA in PBS cells were resuspended in 10 mM Tris–HCl pH 7.5/15 mM NaCl containing 100 μg/ml RNase and incubated at room temperature for 15 min before adding 50 μg/ml PI. Samples were analysed on a FACs Vantage SE (Becton Dickinson, UK) and analysed using CellQuest software. Experiments were performed independently three times.

2.9. Activated caspase-3/PI

Cells were fixed in pre-chilled 1× Fixation Solution (16× Fixation Solution: 37% formaldehyde containing 10% methanol), the cell pellet resuspended in 0.1% Triton X-100 in PBS (300 μl) with anti-active caspase 3 FITC-conjugated antibody (10 μl) (R&D Systems, UK) then incubated at room temperature, protected from light, for 1 h using a rotary mixer. To the cells 0.1% Triton X-100 (Sigma, UK) in PBS (400 μl) was added before pelleting the cells at 4000 rpm/2 min using a bench-top microfuge. The supernatant was removed and the cells stained with PI as described previously for Histone H3 (ser^{10}).

2.10. λH2A.X

Cells were fixed in pre-chilled 1× Fixation Solution (16× Fixation Solution: 37% formaldehyde containing 10% methanol). 1.5×10^6 fixed cells were resuspended in 1× Permeabilisation Solution (300 μl) (10× Permeabilisation Solution components: 5% saponin (Sigma, UK); 100 mM HEPES pH 7.4 (Sigma, UK); 1.4 M $NaCl_2$ (Fisher); 25 mM $CaCl_2$ (Sigma): filtered through 0.2 μm sieve) with anti-phospho-H2A.X FITC-conjugated antibody (10 μl) (Upstate Biotechnology, USA) and incubated at room temperature, protected from light, for 30 min using a rotary mixer. To the cells 1× Wash Solution (400 μl) (10× Wash Solution components: 1% saponin in PBS) was added before pelleting the cells at 4000 rpm/2 min using a bench-top microfuge. The supernatant was removed and the cells stained with PI as described previously for Histone H3 (ser^{10}).

2.11. In vivo complex of enzyme (ICE) assay

The ICE assay was performed as described previously (Osheroff and M.-A. Bjornsti [23]). Briefly, cells were seeded at 3×10^6 cells per 15 cm dish (two dishes per treatment) and allowed to adhere overnight. The cells were then exposed to the drugs for 1 h, collected and lysed with 1 ml 1% sarkosyl in TE buffer (10 mM Tris–HCl pH 8.0, 1 mM EDTA). The cell lysates were then placed onto the top of a preformed caesium chloride step gradient of 1.82, 1.72, 1.50 and 1.37 g/ml in 14 mm × 89 mm polyallomer tubes (Beckman Coulter, UK Ltd.) (2 ml volume for each step gradient). Samples were then subjected to centrifugation at 20 °C in a Beckman SW41 rotor at 30,000 rpm for 24 h. The bottom of the tube was then pierced and 0.5 ml fractions collected. A 200 μl aliquot of each fraction was diluted with an equal volume of 25 mM sodium phosphate buffer pH 6.5 (7.6 ml 1 M Na_2HPO_4 and 17.4 ml 1 M NaH_2PO_4 in 1 L) and applied onto pre-soaked (25 mM sodium phosphate buffer pH 6.5 for 15 min) Protran® nitrocellulose membranes using a slot blot vacuum manifold. Membranes were washed with sodium–phosphate buffer and immunoblotted with an anti-human topoisomerase I antibody. The DNA content of each fraction was visualised by agarose gel electrophoresis.

2.12. Gel filtration

Superose 6 (Amersham Biosciences, UK) 10 cm mini columns, columns were equilibrated with two column volumes of the eluant buffer, 0.01 M Tris HCL pH 8. The columns were then calibrated using protein standards thyroglobulin (MW 669 kDa), phenol red (MW 353 Da) and dextran blue (Sigma, UK) (2 MDa). The protein standards were eluted from the column with eluant buffer, and 0.5 ml fractions of the elute collected. Absorbance at 570 nM and 620 nM of the fractions were read to detect phenol red and dextran blue respectively. To detect thyroglobulin 100 μl aliquots of the fractions were applied onto pre-soaked (with eluant buffer) Protran® nitrocellulose membrane using a slot blot vacuum manifold. The membrane was then stained with Ponceau S (Sigma, UK), imaged on a Fluor-S MultiImager System and analysed using QuantityOne® software.

HCT116 cells were seeded at a density of 3×10^6 per 150 mm culture dish and exposed to GA (1.3 μM) and TPT (213 nM) alone and in combination. Cells were then lysed in RIPA buffer and incubated on ice for 30 min, then cleared by sonication and centrifugation at 14,000 × *g* for 30 min at 4 °C. Forty micro grams of protein from each of the lysate samples was subjected to gel filtration on the sephadex 6 (Sigma, UK) 10 cm mini columns and eluted with eluant buffer. The elute was collected in 0.5 ml fractions; two hundred microlitre aliquots of the fractions were applied onto pre-soaked (eluant buffer) Protran nitrocellulose membrane using a slot blot vacuum manifold. Membranes were then equilibrated with 1× TBST for 15 min at room temperature, then immunoblotted with an anti-human apaf1 antibody (Upstate).

2.13. Statistical analysis

For statistical analysis between drug treatments a comparison of means was performed on the effects of GA and TPT alone and in combination on the HCT116 cell line using one-way ANOVA (data normally distributed). When homogeneity of variance was given the Bonferroni post hoc test was used. For comparison of cell lines comparison of means was performed using one-way ANOVA when data were normally distributed or a Mann–Whitney test when not (SPSS for windows v12.0.1).

2.14. Synergy Determination–Interaction index: isobole method

The interaction index (γ), described by Tallarida [29], is a measure of the degree of synergy or sub-additivity that occurs when two drugs act together. Drug combinations are in fixed ratio proportions; using the formula [drug A in combination]/[drug A alone] + [drug B in combination]/[drug B alone] = γ. If $\gamma = 1$ the interaction is additive, if γ greater than 1 it is sub-additive and if γ is less than 1 it is super-additive (synergistic), as discussed previously [29,31].

Table 1
Concentrations of topoisomerase I and Hsp90 inhibitors alone and in combination required to give 80% inhibition of HCT116 cell growth, interaction indices (γ).

Treatment	Cell type	Single dose TopI inhibitor to give 80% growth inhibition	Single dose Hsp90 inhibitor to give 80% growth inhibition	Combination dose resulting in 80% growth inhibition	γ-Value
TPT + GA	$p53^{+/+}$	15.3 nM	350 nM	8 nM TPT + 50 nM GA	0.67
TPT + GA	$p53^{-/-}$	14.6 nM	350 nM	8 nM TPT + 50 nM GA	0.69
TPT + RD	$p53^{+/+}$	15.3 nM	750 nM	8 nM TPT + 50 nM RD	0.56
TPT + RD	$p53^{-/-}$	14.6 nM	1110 nM	6 nM TPT + 50 nM RD	0.47
IRT + GA	$p53^{+/+}$	4 μM	350 nM	1.5 μM IRT + 125 nM GA	0.73
IRT + GA	$p53^{-/-}$	2 μM	350 nM	0.8 μM IRT + 125 nM 17AAG	0.75
IRT + RD	$p53^{+/+}$	4 μM	750 nM	3 μM IRT + 100 nM RD	0.83
IRT + RD	$p53^{-/-}$	2 μM	1110 nM	0.8 μM IRT + 100 nM RD	0.49
TPT + 17AAG	$p53^{+/+}$	15.3 nM	310 nM	6 nM TPT + 100 nM 17AAG	0.71
TPT + 17AAG	$p53^{-/-}$	14.6 nM	430 nM	6 nM TPT + 100 nM 17AAG	0.64
IRT + 17AAG	$p53^{+/+}$	4 μM	310 nM	0.8 μM + 100 nM 17AAG	0.52
IRT + 17AAG	$p53^{-/-}$	2 μM	430 nM	0.8 μM IRT + 100 nM 17AAG	0.63

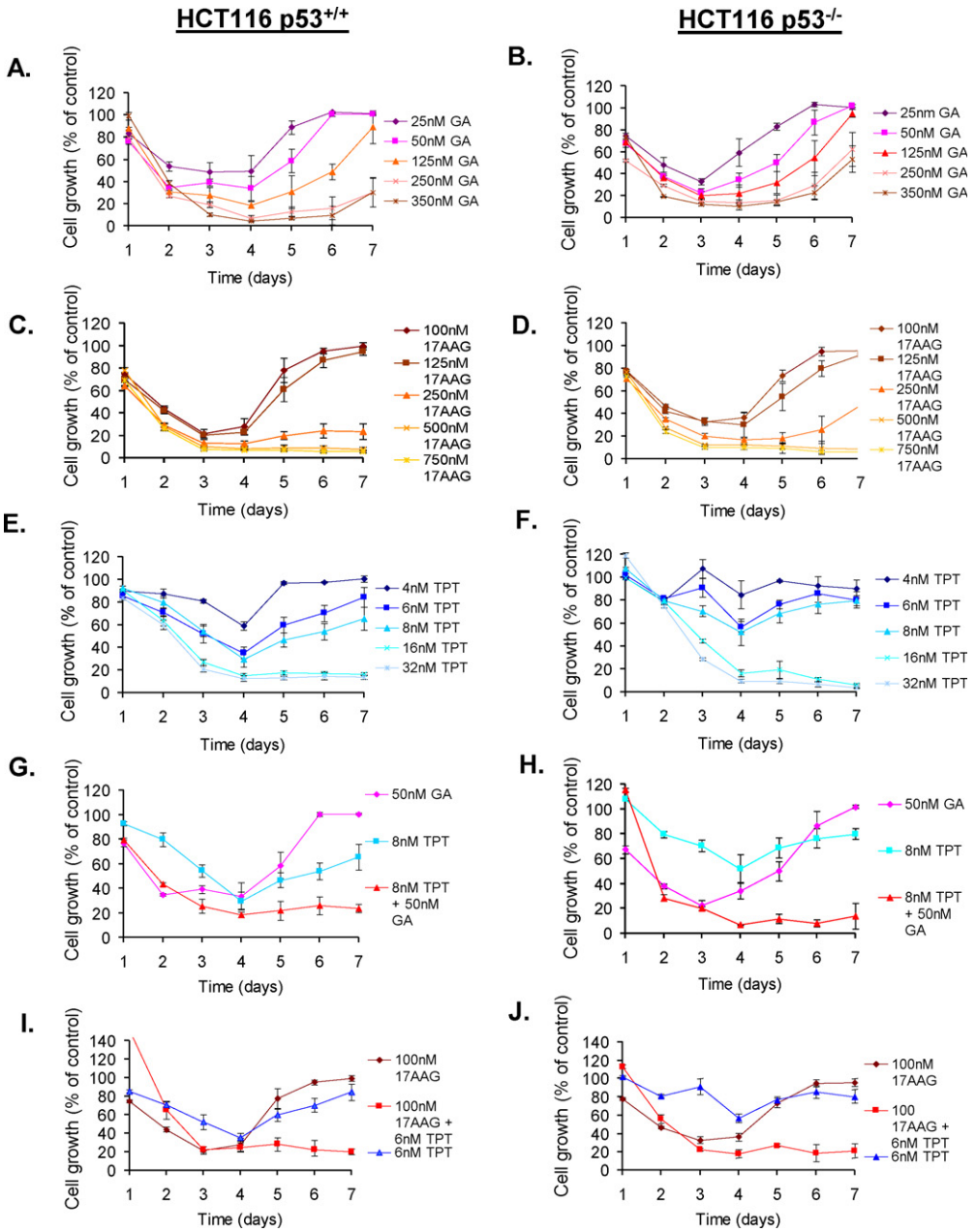

Fig. 1. Proliferation inhibition assays for $p53^{+/+}$ and $p53^{-/-}$ HCT116 cells following dual Hsp90 and topoisomerase I inhibition.
Single dose GA responses in $p53^{+/+}$ (A) and $p53^{-/-}$ (B) cells; single dose 17AAG response in $p53^{+/+}$ (C) and $p53^{-/-}$ (D) cells; single dose TPT response in $p53^{+/+}$ (E) and $p53^{-/-}$ (F) cells; combined GA and TPT response in $p53^{+/+}$ (G) and $p53^{-/-}$ (H) cells; combined 17AAG and TPT response in $p53^{+/+}$ (I) and $p53^{-/-}$ (J) cells. Points represent the average of six replicates; error bars ± SE. 80% proliferation inhibition is achieved in the combination treatments at drug concentrations which when used alone had little effect.

Table 2
Concentrations of topoisomerase I and Hsp90 inhibitors required for LD95, Interaction Indices (γ).

Treatment	Cell type	Single dose Top I inhibitor LD_{95}	Single dose Hsp90 inhibitor LD_{95}	Combination doses LD_{95}	γ-Value
TPT + GA	$p53^{+/+}$	4.1 μM	1.25 μM	169 nM TPT + 1.06 μM GA	0.88
TPT + GA	$p53^{-/-}$	5.05 μM	1.15 μM	115 nM TPT + 0.72 μM GA	0.65
TPT + RD	$P53^{+/+}$	4.1 μM	23.8 μM	640 nM TPT + 16 μM RD	0.83
TPT + RD	$p53^{-/-}$	5.05 μM	21 μM	498 nM TPT + 12.5 μM RD	0.69
IRT + GA	$p53^{+/+}$	245 μM	1.25 μM	29.5 μM IRT + 0.92 μM GA	0.86
IRT + GA	$p53^{-/-}$	256 μM	1.15 μM	23.4 μM IRT + 0.73 μM GA	0.73
IRT + RD	$p53^{+/+}$	245 μM	23.8 μM	106 μM IRT + 13.25 μM RD	0.97
IRT + RD	$p53^{-/-}$	256 μM	21 μM	88.4 μM IRT + 11 μM RD	0.87

3. Results

3.1. Combined topoisomerase I and Hsp90 inhibition cause synergistic inhibition of proliferation

The anti-proliferative effects of combining topoisomerase I and Hsp90 inhibitors were assessed using the sulforhodamine B (SRB) assay, initially developed in 1990 [24] and now widely regarded as a sensitive assay to assess drug induced cytotoxicity [25]. Initial drug screening of the Hsp90 inhibitors GA and 17AAG (Fig. 1A–D) and topoisomerase I poison TPT (Fig. 1E, F) as single agents was used to determine the concentrations of drug to achieve 80% proliferation inhibition (Table 1). In subsequent experiments combined agent treatments the concentration of drugs was decreased in order assess possible synergy. Simultaneous administration of TPT and GA demonstrated synergistic anti-proliferative effects in both $p53^{+/+}$ and $p53^{-/-}$ HCT116 cells (Fig. 1G, H), with 80% proliferation inhibition achieved at drug concentrations which

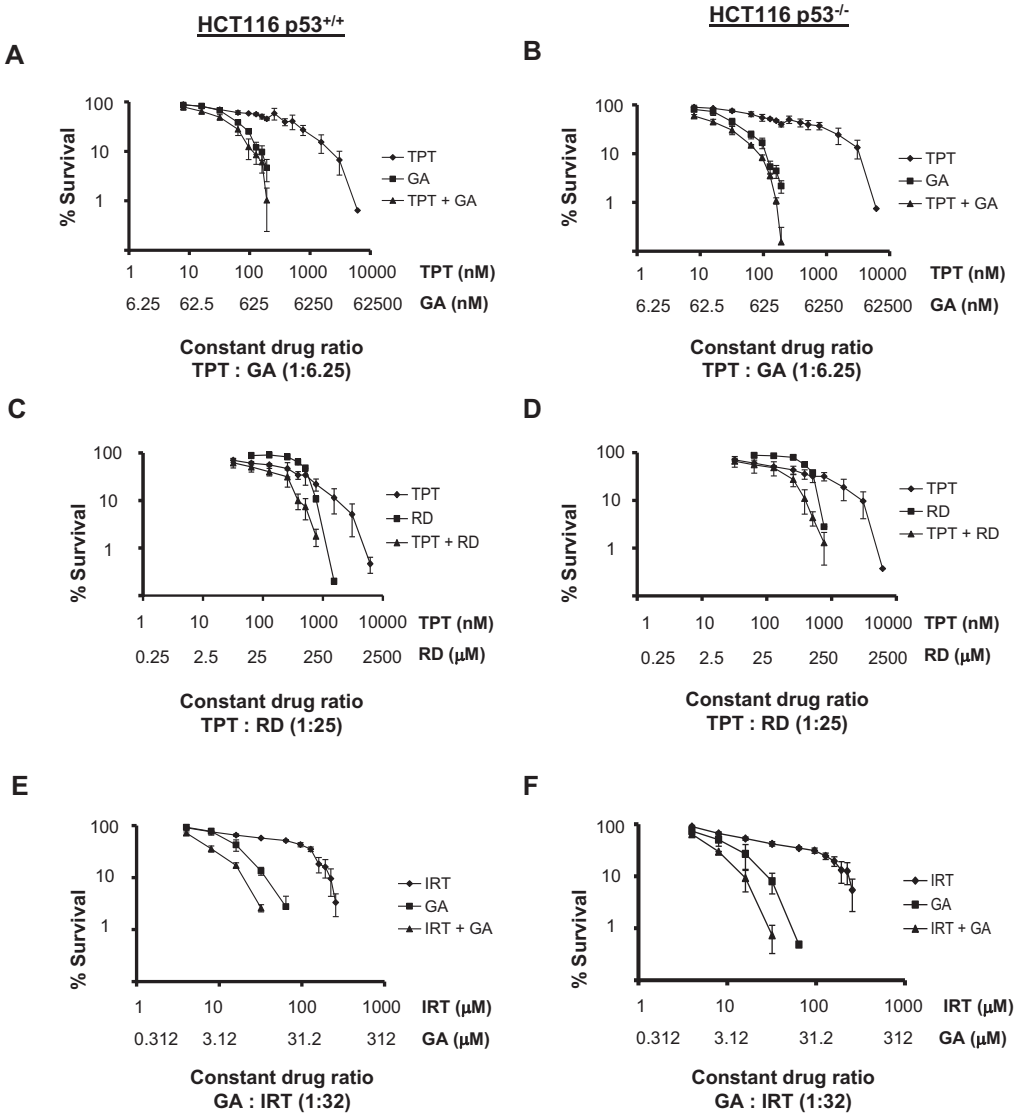

Fig. 2. Clonogenic cell survival curves for $p53^{+/+}$ and $p53^{-/-}$ HCT116 cells following dual Hsp90 and topoisomerase I inhibition using fixed drug ratios.
TPT and GA $p53^{+/+}$ (A) and KO (B) cells; TPT and RD $p53^{+/+}$ (C) and $p53^{-/-}$ (D) cells; IRT and GA $p53^{+/+}$ (E) and $p53^{-/-}$ (F) cells. Ratios between drugs were determined from the SRB proliferation assays with the ratio between the two remaining constant. Points represent the average of at least 3 independent experiments; error bars ± SE. Each drug combination tested displayed synergistic clonogenic survival inhibition for both $p53^{+/+}$ and $p53^{-/-}$ HCT116 cell lines, as confirmed by interaction indices of less than one.

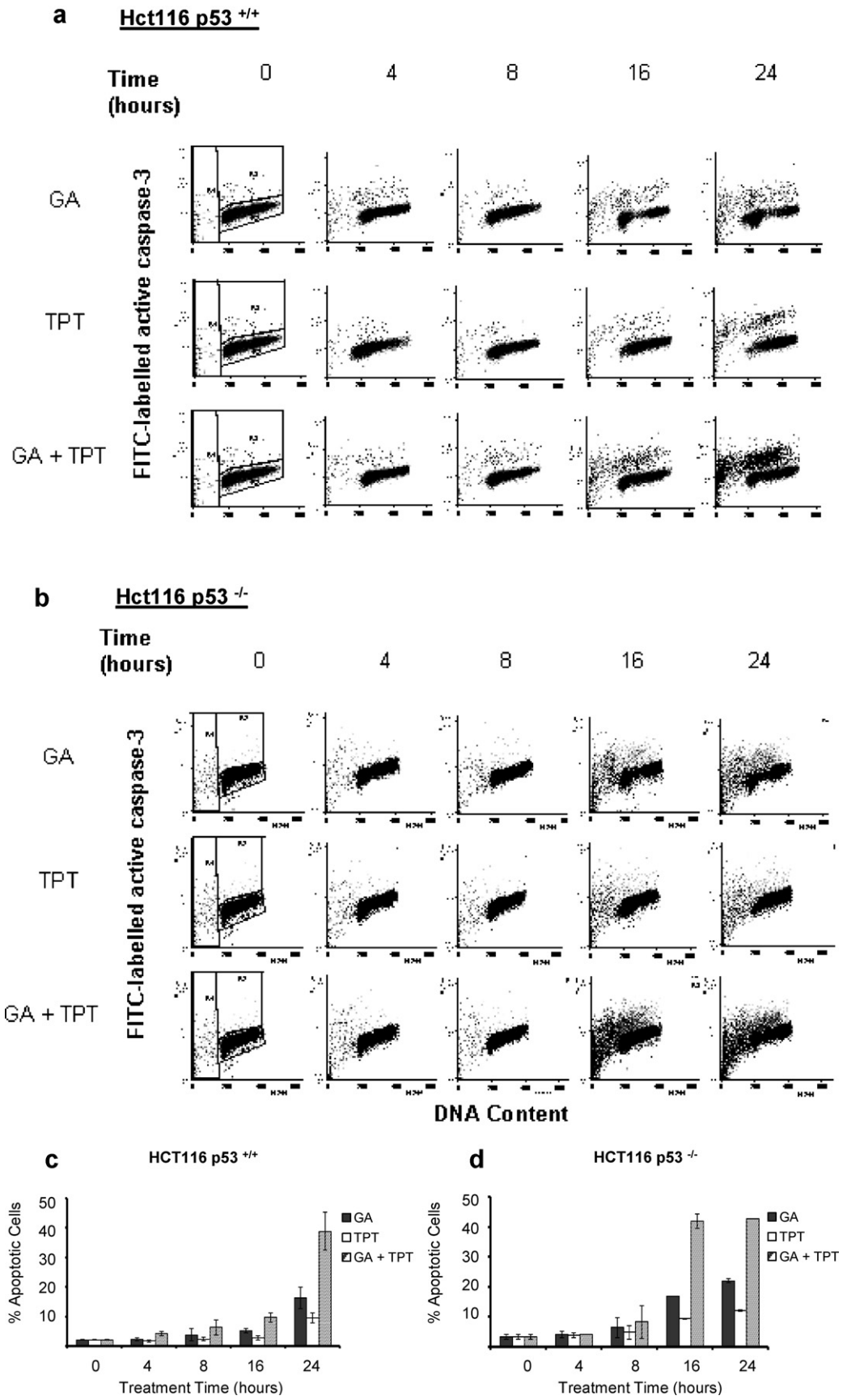

Fig. 3. Combined TPT and GA treatment synergistically enhances apoptosis in both $p53^{+/+}$ and $p53^{-/-}$ HCT116 cells.
FACs analysis of anti-active caspase 3 stained $p53^{+/+}$ (a) and $p53^{-/-}$ HCT116 (b) cells following GA and TPT treatment alone and in combination over a period of 24 h. A greater percentage of cells undergo apoptosis in combined treatment compared to single drugs after 24 h in both $p53^{+/+}$ (c) and $p53^{-/-}$ HCT116 (d) cells. p53 null cells initiate

when used alone had little effect. This phenomenon was further investigated using a variety of combinations; TPT with 17AAG (Fig. 1I, J) and radicicol (RD) (Table 1); IRT with GA, RD and 17AAG (Table 1). All combinations of Hsp90 inhibitors we tested, when used simultaneously with topoisomerase I poisons displayed synergistic inhibition of cell proliferation, in both $p53^{+/+}$ and $p53^{-/-}$ HCT116 cells. Synergy was assessed according to the method of Tallarida [26], where isobolar relationships of less than one confirmed synergy between topoisomerase I poisons and Hsp90 inhibitors.

3.2. Combined topoisomerase I and Hsp90 inhibition cause synergistic cell killing

To assess the effect of the drugs in combination on cell survival we used the clonogenic cell killing assay, a technique widely used to determine the effect of drugs with the potential for clinical application [27]. In the combined treatment both drugs were used in increasing concentrations; ratios between drugs were determined from the SRB proliferation assays with the ratio between the two remaining constant. This strategy has been previously proposed to reduce the number of drug combinations needed to be tested [28].

Fig. 2 demonstrates the effect of TPT and GA alone and in combination on $p53^{+/+}$ and $p53^{-/-}$ HCT116 cell survival. Cell survival curves were plotted on log scale in order to determine the concentration of drugs, alone and in combination, required to generate 95% cell death (LD_{95}) (Fig. 2A, B). To achieve 95% clonogenic inhibition single doses of 4.1 μM TPT and 1.25 μM GA were required for $p53^{+/+}$ and 5.05 μM TPT and 1.15 μM GA for $p53^{-/-}$ cells. These concentrations could be reduced when both drugs were combined with 95% cell death being achieved using 169 nM TPT combined with 1.05 μM GA for $p53^{+/+}$ and 115 nM TPT and 0.72 μM GA for $p53^{-/-}$ cells. These values were used to calculate an isobolar relationship, giving the interaction indices which were 0.88 for $p53^{+/+}$ and 0.65 for $p53^{-/-}$ cells (Table 2). This demonstrates that the combination of TPT with GA has a synergistic cell killing effect at LD_{95} and that this effect is more pronounced in $p53^{-/-}$ cells, having a lower interaction index. Cell survival curves were also plotted for combinations of TPT and RD (Fig. 2C, D) and IRT and GA (Fig. 2E, F). Each of the drug combinations tested displayed synergistic clonogenic survival inhibition for both $p53^{+/+}$ and $p53^{-/-}$ HCT116 cell lines, confirmed by interaction indices of less than one (Table 2). p53 deficient cells (Fig. 2B, D and F) again had lower interaction indices than their wild type counterparts (Fig. 2A, C and E), suggesting increased sensitivity of these cells to the topoisomerase I poison/Hsp90 inhibitor combination.

3.3. Combined topoisomerase I and Hsp90 inhibition synergistically enhances apoptosis

To determine if the mode of cell death induced by the combination treatment was apoptotic we used dual parameter flow cytometry to detect both active caspase-3 and DNA content following drug treatments in both cell lines. The percentage of apoptotic cells was determined by combining the percentage of cells with sub-G1 DNA content and those with activated caspase 3 (Fig. 3).

In $p53^{+/+}$ cells 16 h post treatment, a marginal increase in the percentage of apoptotic cells was detected in the combination treatment compared to single dose GA and TPT. After 24 h

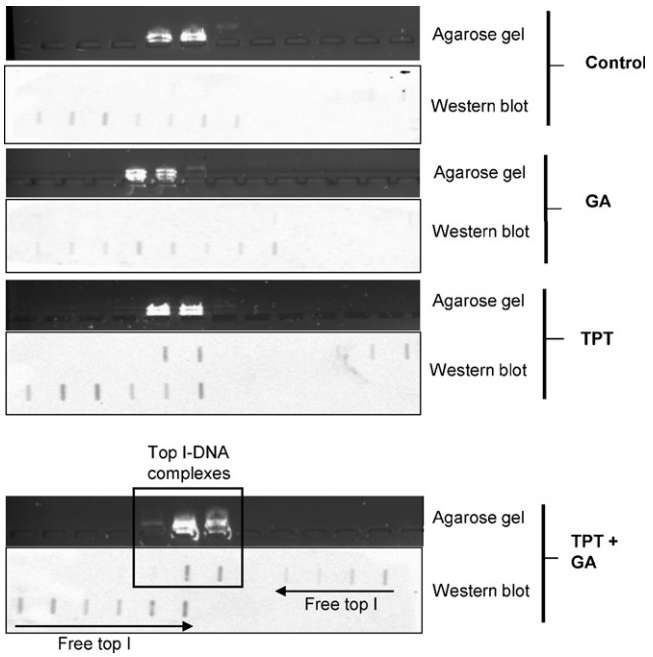

Fig. 4. The effect of drug combinations on the formation of top I–DNA complexes. $p53^{+/+}$ cells were treated with TPT and GA either concurrently or as single agents for 1 h then lysed with 1% sarkosyl, loaded onto a preformed caesium chloride gradient and centrifuged at 30,000 rpm for 24 h. Fractions were then collected and loaded onto nitrocellulose membrane using a slot blot manifold and probed with a topoisomerase I antibody. DNA content of the fractions was determined by gel electrophoresis. Topoisomerase I/DNA complexes were observed in TPT treated cells, however, no increase in complexes was detectable when GA and TPT were used in combination.

combined GA and TPT treatment there was a significantly greater number of cells undergoing apoptosis (39%, mean) compared to either single dose GA (16.4%, mean, $p = 0.017$) or TPT (9.7%, mean $p = 0.003$) (Fig. 3a and c). These results were consistent with time lapse detection of annexin-V which also illustrated enhanced apoptosis in the combined treatment (data not shown). Enhanced apoptosis was also apparent in $p53^{-/-}$ HCT116 cells at both 16 and 24 h time points when there were a substantially increased number of apoptotic cells in the combined GA and TPT treatments compared to the drugs alone (Fig. 3b and d).

In agreement with data from clonogenic cell killing assays, p53 deficient cells appeared more sensitive to the combined GA and TPT treatment with a significantly greater number of apoptotic cells 16 h post treatment (42.1%, mean) compared to their wild type counterparts (9.8%, mean $p = 0.008$). This was a 4.3-fold increase in the number of $p53^{-/-}$ apoptotic cells compared to $p53^{+/+}$ cells at this time point; GA and TPT treatments saw 3.2 and 3.3-fold increases respectively. These data indicate that at this earlier time point GA selectively enhances TPT cytotoxicity through the induction of apoptosis, and that $p53^{-/-}$ cells are preferentially sensitised to this treatment. Twenty four hours post drug treatment there was no significant difference between the percentage of apoptotic $p53^{+/+}$ and $p53^{-/-}$ cells.

3.4. Combined topoisomerase I and Hsp90 inhibition does not cause an increase in topoisomerase I mediated DNA damage

Having established that there was synergy between topoisomerase I and Hsp90 inhibitors in inhibiting both cell proliferation

apoptosis at an earlier time point compared with p53 proficient cells following combined drug treatment. Percentage of apoptotic cells was calculated by amalgamating the percentage of cells with subG1 DNA content with the percentage of active caspase 3 positive cells. Bars are the average of independent experiments $n = 3$ ($p53^{+/+}$) $n = 2$ ($p53^{-/-}$) error bars ± SE.

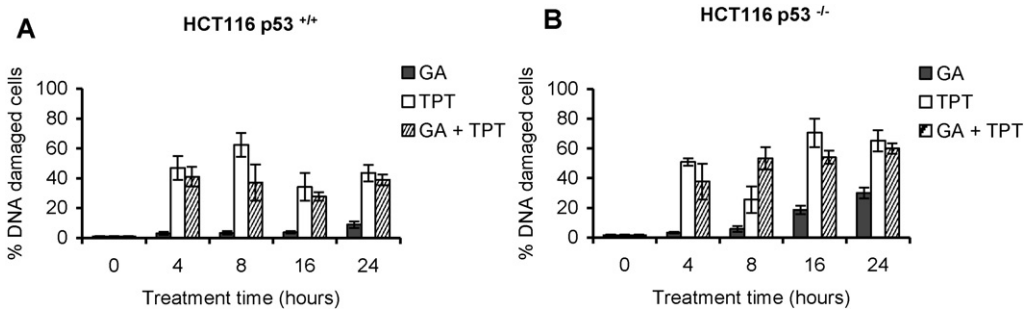

Fig. 5. The effect of drug combinations on the phosphorylation of H2A.X (λH2A.X) in HCT116 $p53^{+/+}$ and $p53^{-/-}$ cells.
$p53^{+/+}$ (A) and $p53^{-/-}$ (B) HCT116 cells were assessed for the presence of λH2A.X following combined and single drug treatments over 24 h. Cells were fixed and labelled with an anti-λH2A.X FITC labelled antibody and analysed using a FACs Vantage SE; percentage of DNA damaged cells was calculated by amalgamating the percentage of cells with subG1 DNA content with the percentage of λH2A.X positive cells. Bars represent the average of at least 3 independent experiments; error bars ± SE. No significant increase in λH2A.X DNA damage was detected in either cell line in combined drug treatment compared to single drugs.

and clonogenic survival mediated via apoptosis, for both $p53^{+/+}$ and $p53^{-/-}$ HCT116 cells, we set out to determine the mechanism behind the synergy.

We have previously reported that combined VP16 and GA treatment results in an increase in topoisomerase II–DNA cleavable complexes in HCT116 cells at 1 h compared with VP16 treatment alone [6]; and speculated that a similar mechanism may also occur following dual TPT and GA treatment. The in vivo complexes of enzyme bound to DNA (ICE) bioassay can be used to measure genomic DNA cleavage mediated specifically by topoisomerase I, by detecting in vivo enzyme complexes bound to DNA. Topoisomerase I DNA complexes are separated from free topoisomerase I protein by gradient centrifugation, then detected using specific antibodies [29]. Using this method we examined topoisomerase I–DNA cleavable complexes 1 h post treatment (Fig. 4). $p53^{+/+}$ HCT116 cells when left untreated or treated with GA contained no topoisomerase I DNA complexes. As expected in TPT treated cells topoisomerase I DNA complexes were present. However, no increase in complexes was detectable when GA and TPT were used in combination.

Double stranded DNA breaks can be detected by the presence of H2A.X phosphorylated at serine 139 (λH2A.X), and analysed by FACs. λH2A.X has been shown to be induced in response to replication mediated dsDNA breaks induced by topoisomerase I cleavage complexes [30,31]. To assess topoisomerase I mediated DNA damage over time we used this assay to compare levels of DNA damage between single and combined GA and TPT treatments.

In both $p53^{+/+}$ and $p53^{-/-}$ HCT116 cells, GA treatment resulted in an increase in λH2A.X immunofluorescence 16 h post drug treatment (Fig. 5A, B). This increase in λH2A.X coincided with an increase in the number of apoptotic cells (Fig. 3) indicating the DNA damage following Hsp90 inhibition was apoptotic. In comparison both single TPT and combined TPT and GA drug treatments showed λH2A.X activation 4 and 8 h post treatment but apoptosis (activated caspase 3) is not detected until 16 h post treatment. It was also evident from FACs scattergrams that at early time points λH2A.X distribution was primarily in S phase cells following TPT treatment alone and in combination with GA (data not shown). At these early time points DNA damage was therefore topoisomerase I mediated and not apoptosis associated DNA fragmentation.

We found no significant increase in phosphorylated λH2A.X in combined GA and TPT treatments compared to TPT treatment alone in either $p53^{+/+}$(Fig. 5A) or $p53^{-/-}$ (Fig. 5B) cells. This data conflicts with the hypothesis of increased topoisomerase I mediated DNA damage being the cause of enhanced apoptosis following dual topoisomerase I and Hsp90 inhibition. We therefore concluded that the synergistic apoptosis seen in $p53^{+/+}$ and $p53^{-/-}$ HCT116 cells following combined TPT and GA treatment (Fig. 3) was not due to increased DNA damage.

3.5. Hsp90 inhibition selectively abrogates the topoisomerase I inhibition induced G2 checkpoint in $p53^{-/-}$ cells

Hsp90 has numerous partner proteins either directly involved in cell cycle progression and/or checkpoints (reviewed in Burrows [32]). We and others have shown that the cell cycle regulatory protein and Hsp90 client, Chk1, is degraded following Hsp90 inhibition [6,22]. Following DNA damage Chk1 plays an important role in the activation and maintenance of the G2/M checkpoint. We

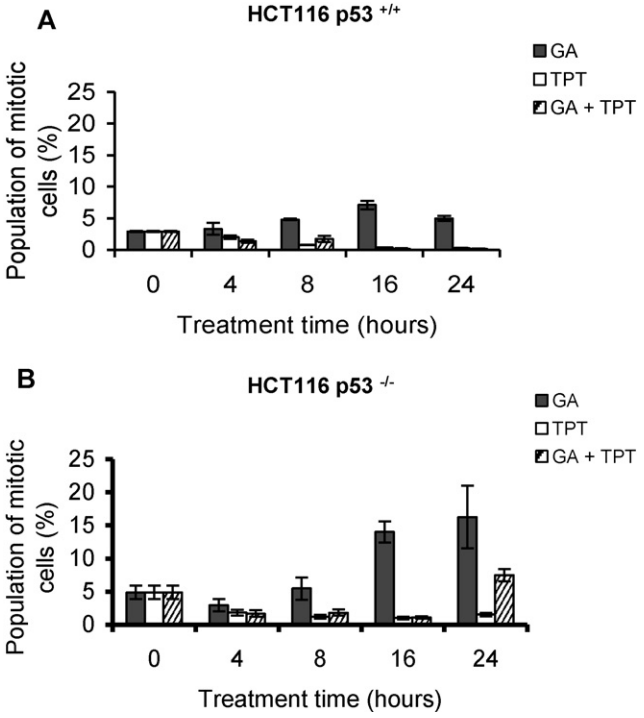

Fig. 6. The TPT induced G2/M checkpoint is abrogated by concurrent addition of the Hsp90 inhibitor GA.
$p53^{+/+}$ (A) and $p53^{-/-}$ HCT116 (B) cells were treated with GA and TPT alone and in combination over 24 h. Cells were fixed and labelled with an anti-phospho histone H3-FITC labelled antibody, stained overnight with PI and analysed using a FACs Vantage SE. Phosphorylated histone H3 fluorescence was associated specifically with mitotic cells and was used to calculate the percentage of mitotic cells. Bars represent the average of at least 3 independent experiments; error bars ± SE.

therefore speculated the integrity of the TPT induced G2/M checkpoint would be compromised with concurrent GA treatment.

Dual parameter flow cytometry was used to analyse DNA content and phosphorylated histone H3 at Ser10, which distinguishes between mitotic and G2 cells [33]. This enabled us to examine the progression of cells from G2 into mitosis following drug treatments. We found no phosphorylation of histone H3 at Ser10 in $p53^{+/+}$ HCT116 cells 24 h post TPT and combined GA/TPT treatment, indicating G2 cell cycle arrest (Fig. 6A). However, in $p53^{-/-}$ HCT116 cells 24 h post combined GA and TPT treatment, phosphorylation of histone H3 at Ser10 was detected demonstrating abrogation of the G2/M checkpoint in these cells (Fig. 6B). Twenty four hour exposure of $p53^{-/-}$ HCT116 cells to TPT alone did not cause abrogation of the G2 checkpoint, proving that checkpoint abrogation in p53 deficient cells was a result of Hsp90 inhibition.

Thus abrogation of the G2/M checkpoint is a probable contributory cause of the enhanced cytotoxicity caused by the combination treatment in $p53^{-/-}$ cells compared to $p53^{+/+}$ cells, in agreement with previous observations [34]. However, it is unlikely that this is the sole mechanism behind the synergy observed in $p53^{-/-}$ cells; apoptosis is synergistically enhanced 16 h post GA and TPT treatment (Fig. 3b and d) prior to the abrogation of the G2 checkpoint occurring after 24 h (Fig. 6B). In addition TPT cytotoxicity was synergistically enhanced by the simultaneous addition of GA in $p53^{+/+}$ cells without abrogation of the G2/M check point, thus there must be an additional underlying mechanism functioning in both $p53^{+/+}$ and $p53^{-/-}$ cells.

3.6. TPT-induced upregulation of the anti-apoptotic protein Bcl2 is reversed by the simultaneous addition of GA

The Bcl2 family of proteins are important in the regulation of the mitochondrial pathway of apoptosis (reviewed in [35,36]. The family consists of both pro-apoptotic and anti-apoptotic members. Anti-apoptotic members include Bcl2 and Bcl_{XL} which are located in the mitochondrial membrane and inhibit the release of apoptosis promoting factors such as cytochrome c [37]. It is believed that the inhibition of apoptosis by oncogenes such as Bcl2 may promote drug resistance in tumours, allowing drug induced damaged cells to evade death. In addition Bcl2 has also been suggested to be a Hsp90 client protein [38–40]. Furthermore GA treatment has been shown to reduced the level of Bcl-2 mRNA and protein expression in a concentration-dependent manner [41]. Taking this into account we investigated whether Hsp90 inhibition

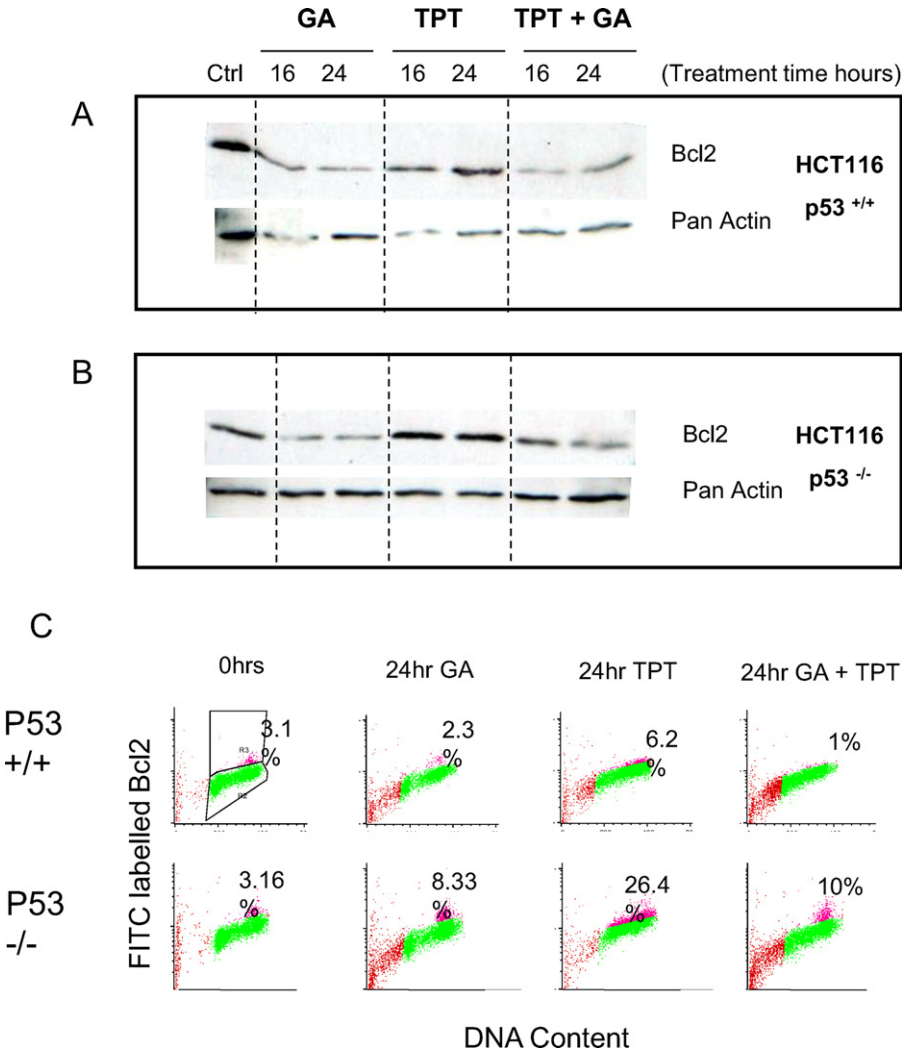

Fig. 7. TPT-induced upregulation of the anti-apoptotic protein Bcl2 is reversed by the simultaneous addition of GA.
$p53^{+/+}$ and $p53^{-/-}$ cells were treated with TPT and GA either concurrently or as single agents for 16 and 24 h then lysed. Cell lysates were separated on a 10% SDS-polyacrylamide gel and subsequent western blots probed with a Bcl2 antibody (Sigma), and loading control beta actin. $p53^{+/+}$ (A), $p53^{-/-}$ (B).
$p53^{+/+}$ and $p53^{-/-}$ HCT116 cells were treated with GA and TPT alone and in combination for 16 and 24 h (C). At the set time points cells were fixed and labelled with an anti-Bcl2 antibody then stained overnight with PI. Cells were analysed using a FACs Vantage SE.

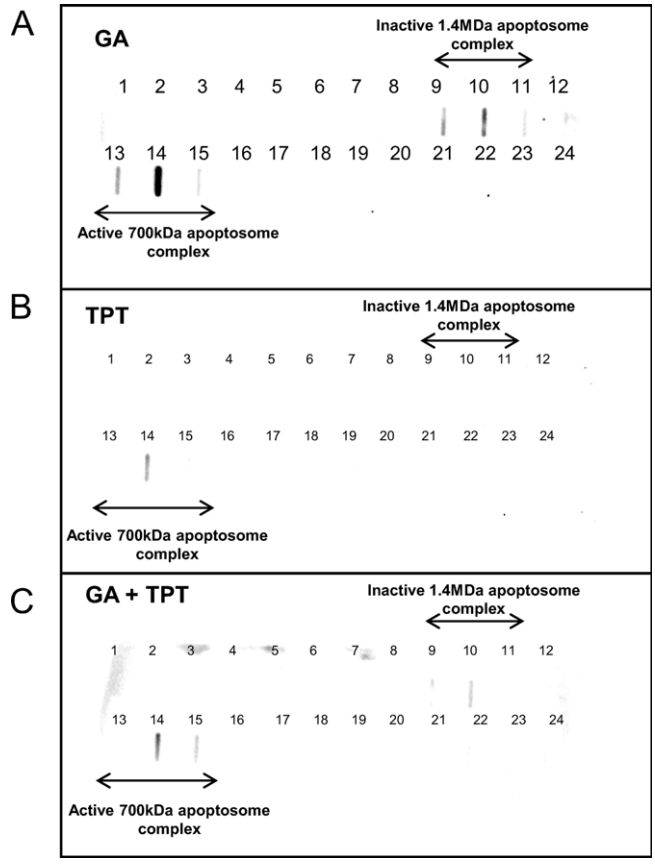

Fig. 8. Hsp90 inhibition results in the formation of two large ~1.4-MDa and ~700 kDa apoptosome complexes.
$p53^{+/+}$ HCT116 cells were treated with TPT and GA either concurrently or as single agents for 24 h, then lysed and 40 μg of protein applied to sepharose 6 10 cm mini columns. Proteins were eluted, fractions collected and applied onto nitrocellulose and probed with an anti-apaf-1 antibody (A) GA (B) TPT (C) GA + TPT.

may lead to a reduction in Bcl2 levels in combined GA and TPT treated cells compared to single TPT treatment.

$p53^{+/+}$ and $p53^{-/-}$ HCT116 cells were treated with TPT and GA alone and in combination over a period of 24 h and subjected to western blot analysis using an anti-Bcl2 antibody. Fig. 7A shows that in both $p53^{+/+}$ and $p53^{-/-}$ cells TPT treatment induces Bcl2 protein expression. However the simultaneous addition of GA with TPT is able to reverse this induction and Bcl2 is degraded (Fig. 7A, B). These results are consistent with FACs analysis which also shows decreased Bcl2 labelling in cells treated with GA alone and in combination with TPT compared with TPT treatment alone (Fig. 7C).

3.7. Effect of Hsp90 inhibition on apoptosome formation

Hsp90 is known to inhibit cytochrome c mediated oligomerisation of Apaf-1 into the active apoptosome, thereby preventing activation of caspase-9 and in turn caspase-3. Depletion of Hsp90 relieved its inhibitory effect on apoptosome formation [42]. With this in mind we assayed for the 700-kDa Apaf1 complex, capable of processing and activating effector caspases [43]. We speculated that in addition to removal of the anti-apoptotic protein Bcl2 the synergy could also be due to the loss of the inhibitory effect of Hsp90 on apoptosome formation, leading to enhanced apoptosis following dual Hsp90 and topoisomerase I inhibition.

Gel filtration was used to separate the 700-kDa active apoptosome from its 1.4-MDa inactive form in cell extracts from $p53^{+/+}$ HCT116 cells treated with the drugs alone and in combination. Protein standards dextran blue (MW 2-MDa), thyroglobulin (MW 678 kDa) and phenol red (MW 376 Da) were used to calibrate Superose 6, 10 cm mini columns; peak intensities of each standard were determined and found to be fraction 9, 13 and 20 respectively (data not shown). Cell lysates from each drug treatment were applied in equal concentrations to columns and eluted. Fractions were collected and applied onto nitrocellulose membrane by means of a slot blot manifold. The presence of apaf-1 was then tested for using an apaf-1 antibody. Following GA treatment apafapafapafapafapaf-1 was detected in fractions 9, 10 and 11 (Fig. 8A) corresponding to fractions that eluted dextran blue, indicating the presence of the inactive 1.4 MDa apoptosome complex. The 700 kDa active apoptosome complex was observed in fractions 13 and 14 in greater amounts than the inactive form indicating a pro-apoptotic status. Only the 700 kDa active form could be detected in the TPT treated cells, but at a reduced level compared to GA treated cells (Fig. 8B). In combined GA and TPT treated cell extracts the inactive 1.4 MDa apoptosome complex could be weekly detected in fraction 10 and the active form 700 kDa was detected in fractions 14 and 15 at higher levels than TPT only treatment but lower than GA alone (Fig. 8C). Thus, it is possible that in combined GA and TPT treated cells Hsp90 inhibition has removed an active apoptosome suppressor, leading to increased apoptosome formation and subsequent apoptosis.

4. Discussion

To resolve the conflict in the literature and generate a more complete understanding of combining clinically useful topoisomerase I poisons with Hsp90 inhibitors we used a number of inhibitors for both targets over a range of concentrations, assessing the apoptotic effect on both $p53^{+/+}$ and $p53^{-/-}$ HCT116 cells.

In agreement with published data we found that $p53^{-/-}$ HCT116 cells displayed increased sensitivity to the topoisomerase I inhibitor IRT compared to their $p53^{+/+}$ counterparts [44,45]. This was observed in both clonogenic cell killing (Fig. 2E and F) and proliferation assays (Table 1). Cell death assessed by the clonogenic assay was significantly increased in $p53^{-/-}$ cells compared to $p53^{+/+}$ cells at low concentrations of IRT. This sensitivity was substantiated by a 4-fold increase in IRT concentration required to achieve LD_{50} in $p53^{+/+}$ compared to $p53^{-/-}$ HCT116 cells. No significant difference in cell death was seen between the cell types at higher concentrations. This observation was supported by the comparable LD_{95} values for $p53^{+/+}$ and $p53^{-/-}$ cells being 245 μM and 256 μM IRT respectively (Table 2). This data corroborates reports finding an increase in sensitivity of $p53^{-/-}$ cells at low concentrations of topoisomerase I poisons but not at high concentrations [46]. Treatment of $p53^{-/-}$ and $p53^{+/+}$ HCT116 cells with a high concentration of CPT resulted in apoptosis, whilst low concentration CPT treatment resulted in apoptosis of $p53^{-/-}$ cells but long term senescence of $p53^{+/+}$ cells [47,46]. This strongly suggests that increased sensitivity to topoisomerase I inhibitors observed in $p53^{-/-}$ cell lines compared to their $p53^{+/+}$ counterparts may be influenced by drug concentration. This may be a contributing factor to the conflicting data available in regard to the protective effects of p53 following topoisomerase I inhibitor treatment.

In contrast to the increased cell killing observed in $p53^{-/-}$ HCT116 cells following treatment with IRT, we found that the p53 status of HCT116 cells did not have an effect on sensitivity to the topoisomerase I inhibitor TPT (Fig. 2A–D). These findings are in agreement with another study which found p53 status to have no influence on sensitivity of glioma cells to TPT treatment [48]. Conversely p53 deficient mouse embryonic fibroblasts have been shown to be significantly more sensitive to TPT than wild-type cells [49]. Whilst as a second line therapy for advanced ovarian

carcinoma patients with $p53^{+/+}$ tumours had a better response to second line TPT therapy, however, mutations in p53 were associated with low responsiveness [50]. These findings suggest that the sensitivity of p53 deficient cells to topoisomerase I poisons may also be cell type specific in addition to any drug dose dependency.

We have clearly demonstrated that Hsp90 inhibitors can sensitise cells to topoisomerase I poisons with both $p53^{+/+}$ and $p53^{-/-}$ status. Synergistic increases in cell death and proliferation inhibition were observed in both $p53^{+/+}$ and $p53^{-/-}$ cells following combination treatments with several topoisomerase I and Hsp90 inhibitors. To further explore the mechanism behind the synergy, we focused on using a single combination of drugs, GA and TPT. Using this drug combination synergy was confirmed to be a result of enhanced apoptosis which occurred at an earlier time point in $p53^{-/-}$ cells. These observations are supported by a previous study where concurrent 17AAG and SN-38 treatment synergistically enhanced cell death in $p53^{+/+}$ HCT116 cells [51]. However it is at odds with another study reporting combined 17AAG and SN-38 treatment synergistically enhanced apoptosis in $p53^{-/-}$ cells but was ineffective at causing apoptosis in $p53^{+/+}$ cells [52]. The discrepancy between these observations can potentially be explained by the conflicting data available with regard to p53 status and sensitivity to topoisomerase I poisons, highlighting the importance of both the concentration and the ratio of drugs in treatments; Recent studies have stressed the need for the evaluation of drug combinations over a wide range of concentrations and ratios, given that a particular ratio of agents can be antagonistic or additive whilst others synergistic [53]. In addition this also stresses the significance of an underlying mechanism behind the synergy that is p53 independent.

We and other groups have previously shown that Hsp90 inhibitors sensitise cells to topoisomerase II inhibitors [54,55]. In addition we have demonstrated that a potential mechanism behind this synergy is increased topoisomerase II mediated DNA damage [6]. It was plausible that a similar mechanism could also apply to the sensitisation of topoisomerase I poisons by Hsp90 inhibitors. However, we did not observe any increase in topoisomerase I mediated DNA damage following dual Hsp90 and topoisomerase I inhibition, compared to single topoisomerase I poison treatments (Fig. 4). Furthermore, FACs analysis for the presence of DNA damage as measured by λH2A.X in drug treated cells confirmed there was no significant difference in DNA damage between drug treatments up to 24 h post treatment in either $p53^{+/+}$ or $p53^{-/-}$ cells (Fig. 5A and B respectively).

Abrogation of cell cycle check point(s) has been suggested as the mechanism behind the synergy observed following dual Hsp90 and topoisomerase I inhibition, based on depletion of Chk1 mediated by Hsp90 inhibition [21]. We and others have also shown depletion of Chk1 following Hsp90 inhibition [6]. We have shown $p53^{+/+}$ cells maintained G2/M checkpoint integrity following combined GA and TPT treatment, verified by reduced phosphorylation of histone H3 (Fig. 6A). However in $p53^{-/-}$ cells we established abrogation of the G2/M checkpoint, confirmed by increased phosphorylated histone H3 (Fig. 6B). We propose that abrogation of the G2/M checkpoint was in part responsible for the increased sensitivity of $p53^{-/-}$ cells to the combination treatment in agreement with published data [34]. The caveat to this being the timing of increased caspase activation in $p53^{-/-}$ cells following the combination treatment at 16 h, which is prior to the increased phosphorylated of histone H3 seen at 24 h. In addition because the dual combination induces apoptosis in both $p53^{+/+}$ and $p53^{-/-}$ cells there must be an additional mechanism responsible for the synergy observed in both cell lines following dual Hsp90 and topoisomerase I inhibition. Studies using the Chk1 inhibitor UCN-01 in combination with camptothecin have demonstrated abrogation of the cell cycle check point leading to slippage and detectable increase in ploidy of the cells about to undergo apoptosis [2]. In our studies using combinations of TPT and GA, no increase in the nuclear content of the cells was observed. This highlights the complexity of compounds that inhibit Hsp90 which target more than one protein/pathway.

The literature describes four main processes that determine the cellular response to topoisomerase I cleavable complexes induced by topoisomerase inhibitors:- [1] Cellular drug accumulation, primarily under the control of the ATP binding drug transporter ABCG2 (also known as breast cancer resistance protein BCRP); [2] DNA repair; [3] growth arrest linked to cell cycle checkpoints; and [4] apoptosis [12]. The latter 3 are downstream of the drug induced topoisomerase I cleavable complexes and each response involves the cooperation of a number of key regulatory proteins and pathways which initiate and/or maintain each process. Rationally designed combination therapies combining agents that deregulate one or other of these pathways with topoisomerase I inhibitors have given promising results [56–58]. Here we report a combination therapy at clinically relevant concentrations that targets at least two of the 4 main pathways activated in response to topoisomerase I inhibition. The therapeutic exploitation of multiple pathways mediated by Hsp90 inhibition confers a distinct advantage as tumour resistance to a therapy that targets multiple proteins and pathways would be more difficult than one targeting a single protein [59].

Dual Hsp90 and topoisomerase I inhibition leads to the deregulation of proteins involved in both the apoptotic and cell cycle response to topoisomerase I cleavable complexes. Based on our observations and the literature we propose a complementary hypothesis: Hsp90 inhibitors sensitise both $p53^{+/+}$ and $p53^{-/-}$ cells to TPT via the activation of pro apoptotic factors, e.g. active apoptosome complexes (Fig. 8) [42] and/or the inhibition of anti apoptotic factors such as Bcl2 that are known to be associated with Hsp90 [38–40] (Fig. 7). This hypothesis is supported by findings that suppression of Bcl2 and Bcl_{XL} substantially increased the efficacy of the topoisomerase I poison CPT treatment both in vitro, in a human ovarian cancer cell line (A2780) and in vivo in human ovarian carcinoma xenografts [60]. Thus, it is possible in TPT treated cells elevated Bcl2 expression suppresses apoptosis and that simultaneous addition of an Hsp90 inhibitor removes this suppression, enhancing apoptosis in combined GA and TPT treated cells.

Combining Topoisomerase I poisons with Hsp90 inhibitors represent real clinical potential, given their efficacy in both p53 wild type and p53 deficient tumours. Furthermore this combination therapy may be particularly useful in cases where chemoresistance has developed to conventional therapies, due to overexpression of Bcl2 and/or apoptosome inhibition. Further work is needed to follow up our observations; an in vivo study using the combination would strengthen the findings and add more weight to any proposed clinical use.

5. Funding

This work was supported by The Medical Research Council; The North West Cancer Research Fund Grant; and The Royal Liverpool and Broadgreen University Hospitals NHS Trust R&D support fund.

Acknowledgements

We thank Dr Sabine Przemeck for performing statistical analysis, Prof. B. Vogelstein The Johns Hopkins Oncology Centre for the HCT116 cell lines and Dr R.J. Schultz, Drug Synthesis and Chemistry Branch, Developmental Therapeutics Program, National Cancer Institute (Rockville, MD) NCI for geldanamycin.

Dr's Harper, Greenhalf and Bates for their comments on the draft manuscript.

References

[1] Wang JC. Cellular roles of DNA topoisomerases: a molecular perspective. Nat Rev Mol Cell Biol 2002;3:430–40.
[2] Furuta T, Hayward RL, Meng LH, Takemura H, Aune GJ, Bonner WM, et al. p21CDKN1A allows the repair of replication-mediated DNA double-strand breaks induced by topoisomerase I and is inactivated by the checkpoint kinase inhibitor 7-hydroxystaurosporine. Oncogene 2006;25:2839–49.
[3] Baker NM, Rajan R, Mondragon A. Structural studies of type I topoisomerases. Nucleic Acids Res 2009;37:693–701.
[4] Fortune JM, Osheroff N. Topoisomerase II as a target for anticancer drugs: when enzymes stop being nice. Prog Nucleic Acid Res Mol Biol 2000;64: 221–53.
[5] Barker CR, Hamlett J, Pennington SR, Burrows F, Lundgren K, Lough R, et al. The topoisomerase II-Hsp90 complex: a new chemotherapeutic target. Int J Cancer 2006;118:2685–93.
[6] Barker CR, McNamara AV, Rackstraw SA, Nelson DE, White MR, Watson AJ, et al. Inhibition of Hsp90 acts synergistically with topoisomerase II poisons to increase the apoptotic killing of cells due to an increase in topoisomerase II mediated DNA damage. Nucleic Acids Res 2006;34:1148–57.
[7] Zhang W, Hirshberg M, McLaughlin SH, Lazar GA, Grossmann JG, Nielsen PR, et al. Biochemical and structural studies of the interaction of Cdc37 with Hsp90. J Mol Biol 2004;340:891–907.
[8] Kamal A, Thao L, Sensintaffar J, Zhang L, Boehm MF, Fritz LC, et al. A high-affinity conformation of Hsp90 confers tumour selectivity on Hsp90 inhibitors. Nature 2003;425:407–10.
[9] Hanahan D, Weinberg RA. Hallmarks of cancer: the next generation. Cell 2011;144:646–74.
[10] Workman P, Burrows F, Neckers L, Rosen N. Drugging the cancer chaperone HSP90: combinatorial therapeutic exploitation of oncogene addiction and tumor stress. Ann N Y Acad Sci 2007;1113:202–16.
[11] Pommier Y, Leo E, Zhang H, Marchand C. DNA topoisomerases and their poisoning by anticancer and antibacterial drugs. Chem Biol 2010;17:421–33.
[12] Pommier Y. Topoisomerase I inhibitors: camptothecins and beyond. Nat Rev Cancer 2006;6:789–802.
[13] Nelson WG, Kastan MB. DNA strand breaks: the DNA template alterations that trigger p53-dependent DNA damage response pathways. Mol Cell Biol 1994;14:1815–23.
[14] Shao RG, Cao CX, Shimizu T, O'Connor PM, Kohn KW, Pommier Y. Abrogation of an S-phase checkpoint and potentiation of camptothecin cytotoxicity by 7-hydroxystaurosporine (UCN-01) in human cancer cell lines, possibly influenced by p53 function. Cancer Res 1997;57:4029–35.
[15] Pommier Y, Redon C, Rao VA, Seiler JA, Sordet O, Takemura H, et al. Repair of and checkpoint response to topoisomerase I-mediated DNA damage. Mutat Res 2003;532:173–203.
[16] Siu WY, Lau A, Arooz T, Chow JP, Ho HT, Poon RY. Topoisomerase poisons differentially activate DNA damage checkpoints through ataxia-telangiectasia mutated-dependent and -independent mechanisms. Mol Cancer Ther 2004;3:621–32.
[17] Jones CB, Clements MK, Wasi S, Daoud SS. Sensitivity to camptothecin of human breast carcinoma and normal endothelial cells. Cancer Chemother Pharmacol 1997;40:475–83.
[18] te Poele RH, Joel SP. Schedule-dependent cytotoxicity of SN-38 in p53 wild-type and mutant colon adenocarcinoma cell lines. Br J Cancer 1999;81: 1285–93.
[19] Zhou Y, Gwadry FG, Reinhold WC, Miller LD, Smith LH, Scherf U, et al. Transcriptional regulation of mitotic genes by camptothecin-induced DNA damage: microarray analysis of dose- and time-dependent effects. Cancer Res 2002;62:1688–95.
[20] Daoud SS, Munson PJ, Reinhold W, Young L, Prabhu VV, Yu Q, et al. Impact of p53 knockout and topotecan treatment on gene expression profiles in human colon carcinoma cells: a pharmacogenomic study. Cancer Res 2003;63: 2782–93.
[21] Pourquier P, Gioffre C, Kohlhagen G, Urasaki Y, Goldwasser F, Hertel LW, et al. Gemcitabine (2′,2′-difluoro-2′-deoxycytidine), an antimetabolite that poisons topoisomerase I. Clin Cancer Res 2002;8:2499–504.
[22] Arlander SJ, Eapen AK, Vroman BT, McDonald RJ, Toft DO, Karnitz LM. Hsp90 inhibition depletes Chk1 and sensitizes tumor cells to replication stress. J Biol Chem 2003;278:52572–7.
[23] Bjornsti MA, Osheroff N. Introduction to DNA topoisomerases. Methods Mol Biol 1999;94:1–8.
[24] Skehan P, Storeng R, Scudiero D, Monks A, McMahon J, Vistica D, et al. New colorimetric cytotoxicity assay for anticancer-drug screening. J Natl Cancer Inst 1990;82:1107–12.
[25] Voigt W. Sulforhodamine B assay and chemosensitivity. Methods Mol Med 2005;110:39–48.
[26] Tallarida RJ. The interaction index: a measure of drug synergism. Pain 2002; 98:163–8.
[27] Munshi A, Hobbs M, Meyn RE. Clonogenic cell survival assay. Methods Mol Med 2005;110:21–8.
[28] Tallarida RJ, Stone Jr DJ, Raffa RB. Efficient designs for studying synergistic drug combinations. Life Sci 1997;61:PL 417–25.
[29] Subramanian D, Furbee CS, Muller MT. ICE bioassay. Isolating in vivo complexes of enzyme to DNA. Methods Mol Biol 2001;95:137–47.
[30] Furuta T, Takemura H, Liao ZY, Aune GJ, Redon C, Sedelnikova OA, et al. Phosphorylation of histone H2AX and activation of Mre11, Rad50, and Nbs1 in response to replication-dependent DNA double-strand breaks induced by mammalian DNA topoisomerase I cleavage complexes. J Biol Chem 2003;278:20303–12.
[31] Huang X, Traganos F, Darzynkiewicz Z. DNA damage induced by DNA topoisomerase I- and topoisomerase II-inhibitors detected by histone H2AX phosphorylation in relation to the cell cycle phase and apoptosis. Cell Cycle 2003;2:614–9.
[32] Burrows F, Zhang H, Kamal A. Hsp90 activation and cell cycle regulation. Cell Cycle 2004;3:1530–6.
[33] Juan G, Traganos F, James WM, Ray JM, Roberge M, Sauve DM, et al. Histone H3 phosphorylation and expression of cyclins A and B1 measured in individual cells during their progression through G2 and mitosis. Cytometry 1998;32: 71–7.
[34] Tse AN, Sheikh TN, Alan H, Chou TC, Schwartz GK. 90-kDa heat shock protein inhibition abrogates the topoisomerase I poison-induced G2/M checkpoint in p53-null tumor cells by depleting Chk1 and Wee1. Mol Pharmacol 2009;75: 124–33.
[35] Youle RJ, Strasser A. The BCL-2 protein family: opposing activities that mediate cell death. Nat Rev Mol Cell Biol 2008;9:47–59.
[36] Rautureau GJ, Day CL, Hinds MG. Intrinsically disordered proteins in bcl-2 regulated apoptosis. Int J Mol Sci 2010;11:1808–24.
[37] Yang J, Liu X, Bhalla K, Kim CN, Ibrado AM, Cai J, et al. Prevention of apoptosis by Bcl-2: release of cytochrome c from mitochondria blocked. Science 1997;275:1129–32.
[38] Dias S, Shmelkov SV, Lam G, Rafii S. VEGF(165) promotes survival of leukemic cells by Hsp90-mediated induction of Bcl-2 expression and apoptosis inhibition. Blood 2002;99:2532–40.
[39] Cohen-Saidon C, Carmi I, Keren A, Razin E. Antiapoptotic function of Bcl-2 in mast cells is dependent on its association with heat shock protein 90beta. Blood 2006;107:1413–20.
[40] Du SJ, Li H, Bian Y, Zhong Y. Heat-shock protein 90alpha1 is required for organized myofibril assembly in skeletal muscles of zebrafish embryos. Proc Natl Acad Sci USA 2008;105:554–9.
[41] Du X, Mi R, Qu Q, Qu Y, Yue T. Effects of geldanamycin on expression of Bcl-2 in human cervical cancer HeLa cells. Chin J Clin Oncol 2008;5:113–7.
[42] Pandey P, Saleh A, Nakazawa A, Kumar S, Srinivasula SM, Kumar V, et al. Negative regulation of cytochrome c-mediated oligomerization of Apaf-1 and activation of procaspase-9 by heat shock protein 90. EMBO J 2000;19: 4310–22.
[43] Cain K, Bratton SB, Langlais C, Walker G, Brown DG, Sun XM, et al. Apaf-1 oligomerizes into biologically active approximately 700-kDa and inactive approximately 1.4-MDa apoptosome complexes. J Biol Chem 2000;275: 6067–70.
[44] Gupta M, Fan S, Zhan Q, Kohn KW, O'Connor PM, Pommier Y. Inactivation of p53 increases the cytotoxicity of camptothecin in human colon HCT116 and breast MCF-7 cancer cells. Clin Cancer Res 1997;3:1653–60.
[45] Wang Y, Zhu S, Cloughesy TF, Liau LM. Mischel PS. p53 disruption profoundly alters the response of human glioblastoma cells to DNA topoisomerase I inhibition. Oncogene 2004;23:1283–90.
[46] Magrini R, Bhonde MR, Hanski ML, Notter M, Scherubl H, Boland CR, et al. Cellular effects of CPT-11 on colon carcinoma cells: dependence on p53 and hMLH1 status. Int J Cancer 2002;101:23–31.
[47] Han Z, Wei W, Dunaway S, Darnowski JW, Calabresi P, Sedivy J, et al. Role of p21 in apoptosis and senescence of human colon cancer cells treated with camptothecin. J Biol Chem 2002;277:17154–60.
[48] Schmidt F, Rieger J, Wischhusen J, Naumann U, Weller M. Glioma cell sensitivity to topotecan: the role of p53 and topotecan-induced DNA damage. Eur J Pharmacol 2001;412:21–5.
[49] Tomicic MT, Christmann M, Kaina B. Topotecan-triggered degradation of topoisomerase I is p53-dependent and impacts cell survival. Cancer Res 2005;65:8920–6.
[50] Oggionni M, Pilotti S, Suardi S, Ditto A, Luoni C, Mariani L, et al. p53 Gene status and response to topotecan-containing chemotherapy in advanced ovarian carcinoma. Oncology 2005;69:154–8.
[51] Flatten K, Dai NT, Vroman BT, Loegering D, Erlichman C, Karnitz LM, et al. The role of checkpoint kinase 1 in sensitivity to topoisomerase I poisons. J Biol Chem 2005;280(14):14349–55. Epub 2005 Feb 7.
[52] Tse AN, Sheikh TN, Alan H, Chou TC, Schwartz GK. 90-kDa heat shock protein inhibition abrogates the topoisomerase I poison-induced G2/M checkpoint in p53-null tumor cells by depleting Chk1 and Wee1. Mol Pharmacol 2009;75(1):124–33. Epub 2008 Sep 26.
[53] Mayer LD, Janoff AS. Optimizing combination chemotherapy by controlling drug ratios. Mol Interv 2007;7:216–23.
[54] Blagosklonny MV, Fojo T, Bhalla KN, Kim JS, Trepel JB, Figg WD, et al. The Hsp90 inhibitor geldanamycin selectively sensitizes Bcr-Abl-expressing leukemia cells to cytotoxic chemotherapy. Leukemia 2001;15:1537–43.
[55] Munster PN, Basso A, Solit D, Norton L, Rosen N. Modulation of Hsp90 function by ansamycins sensitizes breast cancer cells to chemotherapy-induced apoptosis in an RB- and schedule-dependent manner. See: Sausville EA. Combining cytotoxics and 17-allylamino, 17-demethoxygeldanamycin: sequence and tumor biology matters. Clin Cancer Res 2001;7:2155–8. [Clin Cancer Res 2001;7:2228–36].

[56] Shi Y, Liu X, Han EK, Guan R, Shoemaker AR, Oleksijew A, et al. Optimal classes of chemotherapeutic agents sensitized by specific small-molecule inhibitors of akt in vitro and in vivo. Neoplasia 2005;7:992–1000.
[57] Tse AN, Klimstra DS, Gonen M, Shah M, Sheikh T, Sikorski R, et al. A phase 1 dose-escalation study of irinotecan in combination with 17-allylamino-17-demethoxygeldanamycin in patients with solid tumors. Clin Cancer Res 2008;14:6704–11.
[58] Houghton PJ, Germain GS, Harwood FC, Schuetz JD, Stewart CF, Buchdunger E, et al. Imatinib mesylate is a potent inhibitor of the ABCG2 (BCRP) transporter and reverses resistance to topotecan and SN-38 in vitro. Cancer Res 2004; 64:2333–7.
[59] Jenkins JR. A proteomic approach to identifying new drug targets (potentiating topoisomerase II poisons). Br J Radiol 2008;81(Spec. No. 1): S69–77.
[60] Dharap SS, Chandna P, Wang Y, Khandare JJ, Qiu B, Stein S, et al. Molecular targeting of BCL2 and BCLXL proteins by synthetic BCL2 homology 3 domain peptide enhances the efficacy of chemotherapy. J Pharmacol Exp Ther 2006;316:992–8.